

## Gopichand Dirisenapu<sup>1\*</sup>, Laxmanaraju Salavaravu<sup>2</sup>, Lingaraju Dumpala<sup>3</sup>

<sup>1</sup> Panchayat Raj Engineering Department, Andhra Pradesh, India

<sup>2</sup> Department of Mechanical Engineering, Sri Sivani College of Engineering, Chilakapalam Jn, Etcherla, India

<sup>3</sup> Department of Mechanical Engineering, Jawaharlal Nehru Technological University, Kakinada, India

\*Corresponding author. E-mail: dchandu310@gmail.com

Received (Otrzymano) 28.05.2023

<https://doi.org/10.62753/ctp.2023.02.4.4>

# INFLUENCE OF EDM PROCESS PARAMETERS OF NOVEL Al7010/B<sub>4</sub>C/BN HYBRID METAL MATRIX NANOCOMPOSITE

In this present research work, the electrical discharge machining (EDM) characteristics of an Al7010/2%B<sub>4</sub>C/2%BN (the reinforcement particles are taken as wt.%) hybrid metal matrix nanocomposite (HMMNC) are discussed. The effect of the EDM process variables like the discharge current ( $I$ ), pulse on time ( $P_{on}$ ), pulse off time ( $P_{off}$ ) and gap voltage ( $V_g$ ) on the response characteristics like the material removal rate (MRR), tool wear rate (TWR), and surface roughness (SR) are presented. The results revealed that the MRR, TWR, and SR grew with an increase in  $I_p$  and  $P_{on}$ . MRR, TWR, and SR increased with a rise in  $P_{off}$  up to 25  $\mu$ s then declined. MRR, TWR, and SR decreased with an increment in gap voltage. The highest MRR was observed for a discharge current of 8 A,  $P_{on}$  of 60  $\mu$ s,  $P_{off}$  of 25  $\mu$ s and  $V_g$  of 30 V. SR and TWR were the smallest at  $I_p$  of 2 A,  $P_{on}$  of 15  $\mu$ s,  $P_{off}$  of 55  $\mu$ s and  $V_g$  of 60 V. The scanning electron microscope (SEM) micrographs of the machined surfaces revealed voids, craters and micro cracks.

**Keywords:** nanocomposites, EDM, material removal rate, tool wear rate, surface roughness

## INTRODUCTION

Aluminium metal matrix nanocomposites (AMMNCs) reinforced with ceramic nanoparticles offer substantial performance benefits over pure aluminium and its alloys. AMMNCs are advanced materials that exhibit exceptional properties such as high strength, low density, corrosion resistance, and excellent electrical and thermal conductivity. These properties make them highly desirable for use in a variety of applications across several industries, including defence, military, aerospace, and automotive. These materials have gained widespread attention due to their unique properties and are expected to continue to grow in popularity as new ways to develop their properties are discovered [1-3]. Common reinforcement particles used in the aluminium matrix are Al<sub>2</sub>O<sub>3</sub>, SiC, B<sub>4</sub>C, TiB<sub>2</sub>, BN, MOS<sub>2</sub>, WC, TiC, and others. These reinforcement particles can be of various sizes ranging from micrometres to nanometres. Nevertheless, the incorporation of micro-sized reinforced particles reduces the fracture toughness and ductility of aluminium metal matrix composites (AMMCs) [4]. Improved ductility and fracture toughness are gained by using nanoparticles in AMMNCs [5]. The preparation of AMMNCs is difficult because of the density variations of nanoparticles concerning aluminium. A limited number of manufacturing techniques are available to prepare AMMNCs, which include ultrasonic-assisted stir casting, squeeze casting, powder

metallurgy, and hot extrusion. Out of the available techniques, ultrasonic-assisted stir casting (UASC) is the preferred method owing to its ability to uniformly disperse nanoparticles in the base alloy by aiding in wetting and distribution [6-8].

The ceramic particles in AMMNCs pose serious problems while machining using conventional methods because of their hardness and brittle nature. Thus, most researchers use unconventional machining processes for machining AMMNCs. Among unconventional machining methods, EDM is extensively used due to its peculiar nature of achieving high dimensional accuracy, cost-effectiveness and capability of producing intricate shapes. EDM is a thermo-electric machining method where the ejection of material happens because of spark energy generated in the gap between the electrode and workpiece (WP) submerged in dielectric fluid.

The EDM process operates independently of the physical and mechanical properties of WP [9]. The selection of suitable EDM process variables is an important factor that improves the machining properties. The output characteristics of the EDM route are MRR, TWR and SR and they are very much dependent on the contributing variables like  $I_p$ ,  $P_{on}$ ,  $P_{off}$  and  $V_g$ . From the literature, it was identified that most researchers concentrated on optimizing the input process parameters to derive maximum efficiency concerning the output characteris-

tics. Velmurugan et al. performed EDM machining on Al6061-10SiC-4Gr hybrid composites and studied the influence of control factors like the current, flushing pressure ( $F_p$ ),  $P_{on}$  and  $V_g$  on SR, TWR and MRR. They found that MRR increases with a rise in  $P_{on}$ ,  $I_p$ , and reduces with improvement in  $V_g$  and  $F_p$ . TWR rises with an increment in  $I_p$ , and  $V_g$ , and falls with an increase in  $F_p$  and  $P_{on}$  [10]. Kumar et al. examined the influence of the input variables like  $I_p$ ,  $P_{on}$ , pulse duty factor ( $\tau$ ), and  $V_g$  on the performance factors of the electrode wear rate (EWR), SR, and power consumption in machining the Al6351/5%SiC/5%B<sub>4</sub>C hybrid composite by EDM processes. The SEM micrographs revealed craters and recast layers on the surface of the composite. Further in their observations, it was reported that the performance factors were significantly affected by  $I_p$ , with an impact of 76.65% to SR, 33.08% to EWR, and 48.08% to power consumption [11]. Senthilkumar et al. determined the influence of  $I_p$  (A),  $P_{on}$  and  $F_p$  on the output parameters of MRR and TWR during the machining of as-sintered Al-TiC MMC with varying wt.% (2.5 and 5) of TiC using EDM. In this process, kerosene was used as the dielectric fluid and the electrode is a 7 mm copper rod. The performances revealed an increased MRR with a rise in the wt.% of TiC particles in the AMMCs. MRR and TWR are affected by  $I_p$ .  $F_p$  plays a significant role in continuing the machining and enhancing MRR at higher  $I_p$  and  $P_{on}$  duration [12]. Jabbaripour et al. determined the effects of the control factors on MRR, TWR and different variables of surface integrity such as the micrographs of the EDMed surfaces and RLT. The study revealed that an increase in  $P_{on}$  led to an enhancement in MRR, but its effect was not as significant as that of  $V_g$  and  $I_p$ . However, TWR increased with  $P_{on}$  and was not significantly affected. On the other hand, an increase in  $I_p$  resulted in an improvement in TWR. Also,  $I_p$  resulted in the formation of pits, micro holes, and surface abnormalities due to the discharge energy, which created larger and deeper craters. As  $P_{on}$  increased, particularly at higher values, the density of microholes and pits, surface cracks, and surface abnormalities also improved as a consequence of arcing. The recast layer exhibited higher microhardness than the hardness of the HAZ and bulk layers, which was attributed to the formation of TiC. Additionally, the hardness of the recast layer was enhanced resulting from the rise in  $I_p$ , which heated the WP surface [13]. Katamreddy et al. examined the influence of  $I_p$ ,  $P_{on}$  and  $F_p$  on SR, MRR, and TWR of an AlB<sub>2</sub> reinforced Al LM25 functionally graded composite. The results revealed that MRR, SR and TWR are highly affected by current. The pulse current played the main role in enhancing MRR and SR, while raising  $P_{on}$  leads to a reduction in TWR [14]. Singh et al. reported on the impact of the EDM factors on the machining of Al/SiC/Gr HMMCs prepared using the SC route. The influences of the process variables like the current,  $P_{on}$  and the tool material are studied on the three performance responses, namely, SR, TWR and MRR.

The best machining outcome was identified at  $I_p$  (10 A),  $P_{on}$  (120  $\mu$ s), and  $V_g$  (4 V) and the copper electrode material exhibited the highest MRR, as well as smallest SR and TWR [15].

From the literature review, it was identified that very little work has been done on analysis of the EDM characteristics of AHMMNCs. The present investigation reveals the influence of the control parameters with different variations such as discharge current (2, 4, 6, and 8 A),  $P_{on}$  (15, 30, 45, 60  $\mu$ s),  $P_{off}$  (10, 25, 40, and 55  $\mu$ s), gap voltage (30, 40, 50, and 60 V) on the machining of a novel Al7010/2%B<sub>4</sub>C/2%BN HMMNC by EDM. The performance characteristics like SR, MRR and TWR were determined. The surface topography of the EDM machined surface was investigated using SEM.

## MATERIALS AND METHODS

### Material preparation

In this paper, Al7010 alloy is the base material and B<sub>4</sub>C and BN nanoparticles as the reinforcement. The Al7010 alloy and the nanoparticles were procured from Paraswamini Metals, Mumbai, India. The Al7010/2%B<sub>4</sub>C/2%BN HMMNC was fabricated using UASC processes.

The process involves the use of various equipment such as an ultrasonic probe, electric resistance heating furnace, transducer, ultrasonic generator, and an inert gas protection system. A graphite crucible with a volume of 1.5 kg was utilized to melt the Al 7010 alloy. The ultrasonic probe, which is made of titanium, generates a frequency of 20 kHz with a power of 2 kW. The Al 7010 alloy, weighing 1 kg, was melted in the graphite crucible at a temperature of 750°C, under the protection of argon gas. The required amount of preheated nanoparticles (B<sub>4</sub>C & BN) was then added to the liquid melt, and the mixture was stirred with a mechanical stirrer at 600 RPM for 25 minutes to create agitation. The ultrasonic probe was then immersed in the melt to a depth of 30 mm from the bottom of the crucible and vibrated for 25 minutes to disintegrate any clustered B<sub>4</sub>C and BN nanoparticles. Afterwards, the stopper was removed from the furnace, and the melt was poured into a mild steel mould that was preheated to 600°C and allowed to solidify. The solidified composites were then cut into standard specimens using wire-cut EDM and their properties were tested. Table 1 provides a summary of the mechanical properties of Al7010/2%B<sub>4</sub>C/2%BN HMMNC.

TABLE 1. Mechanical characteristics of AHMMNC [1]

Composite composition	UTS [MPa]	YTS [MPa]	% Elongation	Micro-hardness [HV]
AA7010-2%B <sub>4</sub> C-2%BN	227.089	218.56	1.022	172.72

**Experimental procedure**

The EDM experiments were conducted using a SPORKONIX EDM S 65 machine and a schematic diagram of EDM processing is presented in Figure 1a, b. The EDM has a servo control system to facilitate upward and downward movement of the electrode and a jet flushing system for flushing the dielectric fluid onto WP and the electrode. The EDM oil is used as dielectric fluid. A cylindrical electrode with a diameter of 10 mm made of pure electrolytic copper with a purity of 99.9% is utilized in the experiment. A rectangular plate with dimensions 120 mm x 60 mm x 6 mm was used as the workpiece material. A machining depth of 1 mm was maintained throughout the experimentation work. The experimental details of EDM are indicated in Table 2.

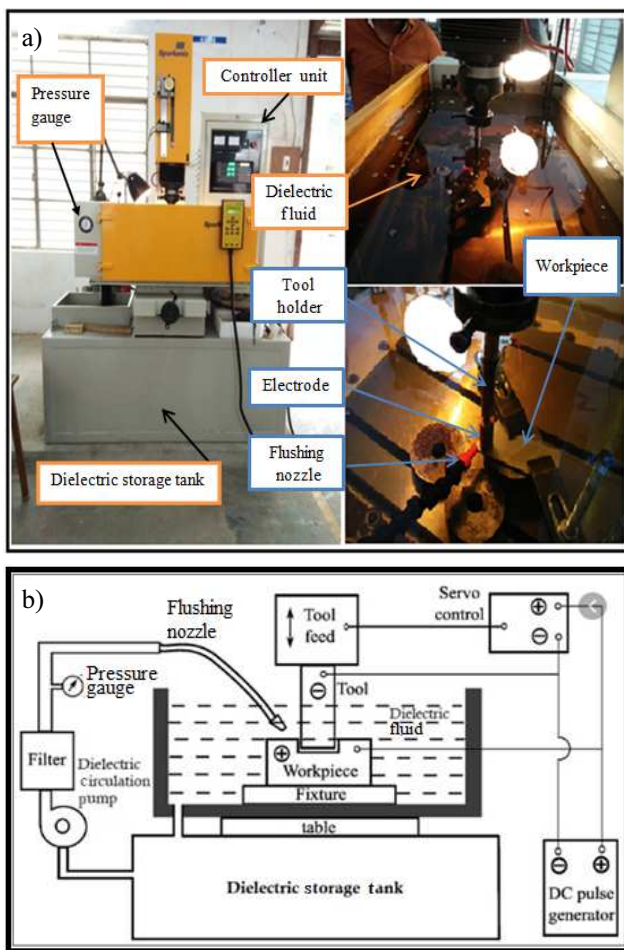


Fig. 1. Electrical discharge machine (a), and schematic diagram (b)

TABLE 2. Experimental details

Experimental data	Specifications
EDM	Sparkonix (Bangalore, India)
Tool	Copper rod (10 mm diameter, 110 mm length)
Flushing pressure	1.25 kg/cm <sup>2</sup>
Dielectric fluid	EDM oil (viscosity CST at 30°C)

SEM, model JEOL, JSM-660LV with EDS was used for the microstructural analysis of the composite material. The XRD analysis of the materials was conducted by means of a PAN analytical Expert Pro diffractometer with a CuK $\alpha$  radiation apparatus.

The experiments were carried out using the one-factor-at-a-time approach by varying the control factors like pulse current (A),  $P_{on}$  ( $\mu$ s),  $P_{off}$  ( $\mu$ s) and  $V_g$  (V) to measure the output characteristics like SR, MRR and TWR. The SR of the machined AHMMNC is measured using a portable surface roughness tester (Talysurf).

MRR is the ratio between the amounts of WP material removed and the machining time, which is calculated using the equation given below. The weight of the material removed during machining is determined using a high precision weighing balance (Shimadzu AUX120) with an accuracy of 0.0001 grams.

MRR and TWR:

$$MRR \text{ (g/min)} = \frac{W_{wb} - W_{wa}}{T_m \text{ (min)}}$$

$$TWR \text{ (g/min)} = \frac{W_{tb} - W_{ta}}{T_m \text{ (min)}}$$

where:  $W_{wb} - W_{wa}$  – weight difference of the workpiece, and  $W_{tb} - W_{ta}$  – weight difference of the tool.  $T_m$  is the machining time.

**RESULTS AND DISCUSSION**

**Microstructure of AHMMNC**

Figure 2a displays the SEM micrograph of Al7010/2%B<sub>4</sub>C/2%BN HMMNC and it reveals uniform dispersion of the B<sub>4</sub>C and BN nanoparticles in Al7010.

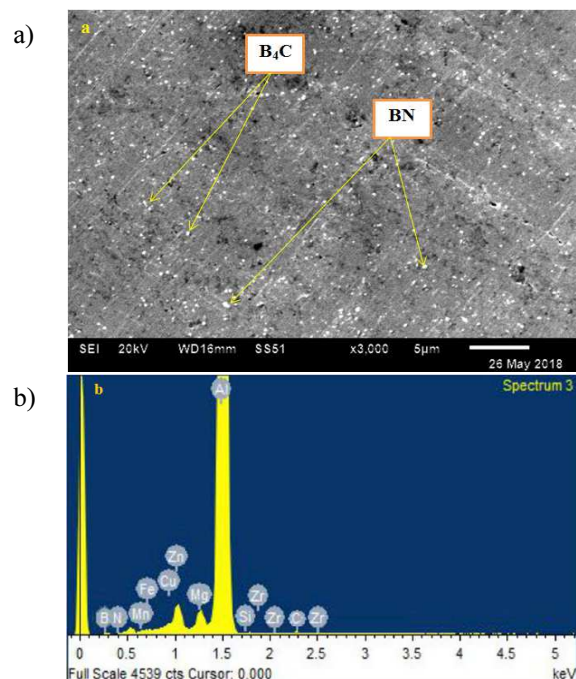


Fig. 2. SEM micrograph and EDS spectrum of Al7010/2%B<sub>4</sub>C/2%BN HMMNC (a-b)

Uniform dispersion of the B<sub>4</sub>C and BN nanoparticles is an important prerequisite to obtaining the optimum mechanical properties in AHMMNC. A lack of casting faults like porosity, and oxide inclusion is also observed in the SEM micrographs. The EDS examination of Al7010/2%B<sub>4</sub>C/2%BN HMMNC is displayed in Figure 2b. The Figure specifies reveals that a high peak of Al alloy and low peaks of boron, carbon and nitrogen were present.

The phase purity of AA7010/B<sub>4</sub>C/BN HMMNC is determined using XRD. The XRD analysis graphs are shown in Figure 3. The results reported the presence of a base matrix observed by strong and long peaks, and B<sub>4</sub>C and BN particles with small peaks. The XRD pattern also shows the purity of AHMMNC without any oxidation reaction during its production.

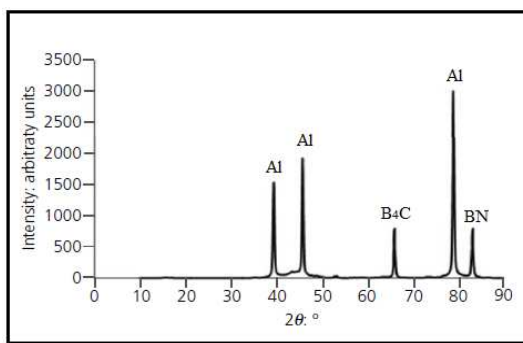


Fig. 3. XRD patterns of Al7010/2%B<sub>4</sub>C/2%BN HMMNC

**Material removal rate (MRR)**

The effect of the control factors on MRR is displayed in Figure 4a-d. With an increase in applied current, MRR grows. The rise in applied current causes increments in the discharge energy and increases the impulsive forces on the machining region of the work-piece, resulting in a higher melting temperature and hence higher MRR. In EDM processes, energy is supplied during  $P_{on}$ .

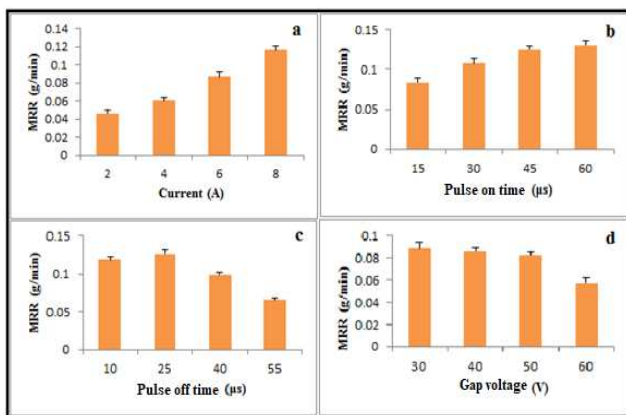


Fig. 4. Influence of EDM process factors on MRR for EDM of AA7010/2%B<sub>4</sub>C/2%BN HMMNC

As  $P_{on}$  grows, more energy is supplied to the work-piece, which raises MRR. This  $P_{on}$  and MRR are pro-

portional to each other. When  $P_{on}$  is increased from 15 µs to 60 µs, the content of energy supplied grows because it produces superior discharge energy, thus increasing the quantity of metal removed from WP [17]. MRR grows with a rise in  $P_{off}$  from 10 µs to 25 µs. With a further increment in  $P_{off}$  from 40 µs to 55 µs, less energy is supplied between the tool and workpiece as output and MRR decreased. MRR drops with arise in  $V_g$  due to reducing in the supply of energy with the increase in  $V_g$  [18]. The machined specimens are shown in Figure 5.



Fig. 5. Machined specimen of nanocomposites

**Tool wear rate (TWR)**

The effect of the various EDM process variables on TWR is presented in Figure 6a-d. Figure 6a reveals that as input  $I_p$  rises from 2 A to 8 A, TWR increases. The increase in  $I_p$  raises the spark discharge energy, and hence increases melting and vaporization of the material from the tool and subsequently increasing TWR. Also, an increment in the current elevates the thermal loading on the tool, which results in high TWR. A Figure 6b display the increased TWR with the rise in  $P_{on}$  which is due to the higher  $P_{on}$ . Heat is applied for a longer time and high heat is formed between WP and the electrode [19].

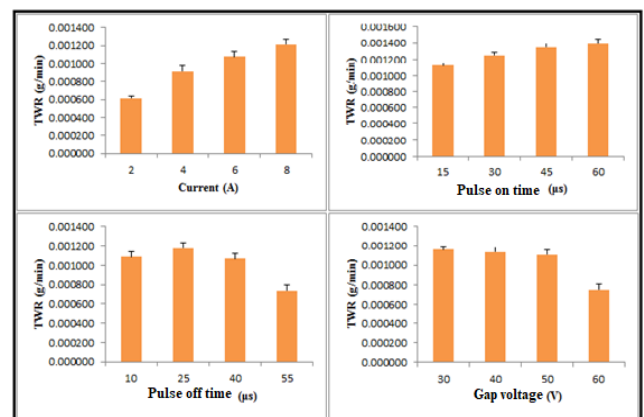


Fig. 6. Influence of EDM process factors on TWR for EDM of AA7010/2%B<sub>4</sub>C/2%BN HMMNC

The influence of  $P_{off}$  on TWR is indicated in Figure 6c. TWR initially increases with the rise in  $P_{off}$

from 10  $\mu$ s to 25  $\mu$ s and later on diminishes with the increase from 40  $\mu$ s to 55  $\mu$ s. The influence of the gap voltage on TWR is displayed in Figure 6d. With the increment in  $V_g$  from 30 V to 40 V TWR increases and beyond that, it decreases. Similar results of the influence of  $V_g$  on TWR are reported in the literature [19].

**Surface roughness (SR)**

Figure 7a-d displays the effect of the EDM process factors on the SR of AHMMNC. The SR of AHMMNC raises with an increase in the applied current as indicated in Figure 7a. The increment in the applied current raises the heat energy and forms a pool of molten material which exists in the overheated form. As an outcome, with rapid growth in the discharge energy, large craters and pockmarks are produced on the surface.

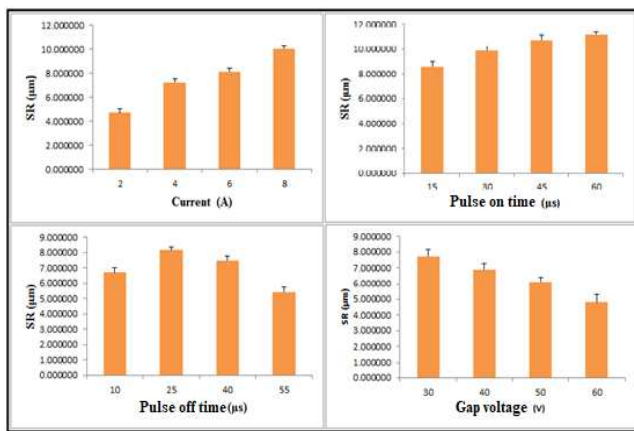


Fig. 7. Influence of EDM process factors on SR of composite

This results in a rise in SR [12]. While  $P_{on}$  is increased from 15  $\mu$ s to 60  $\mu$ s, SR increases and is shown in Figure 7b. This result leads to the creation of an uneven or rough surface because of the increased energy input. The influence of  $P_{off}$  on the SR of the AHMMNC is presented in Figure 7c. With an increase in  $P_{off}$  from 10  $\mu$ s to 25  $\mu$ s, SR grows and with a further increment from 40  $\mu$ s to 55  $\mu$ s SR decreases. As  $P_{off}$  was increased from 10  $\mu$ s to 25  $\mu$ s, a plasma channel formed in the discharge gap is high and the bombarding impulsive forces of energy are high due to the high transfer of ions and increase in SR [11].

With an increase in  $P_{off}$  beyond 25  $\mu$ s, SR decreases, which may be due to less heat, resulting in a lower quantity of material removal. The influence of the gap voltage on the SR of the AHMMNC material is indicated in Figure 7d. With the growth in  $V_g$ , the surface roughness decreased.

**SURFACE MORPHOLOGY**

The SEM micrographs of the EDM machined surface under different conditions of control factors on MRR and SR are displayed in Figure 8. Figure 8a-b shows that the EDM process creates craters, different sizes of cracks and marks of a void. In the EDM route, various particles are removed and enclosed in the surface of the molten material and ejected indiscriminately due to the uneven EDM surface. Input  $I_p$  is the most influential factor and it grows with high discharge energy, creating deeper craters.

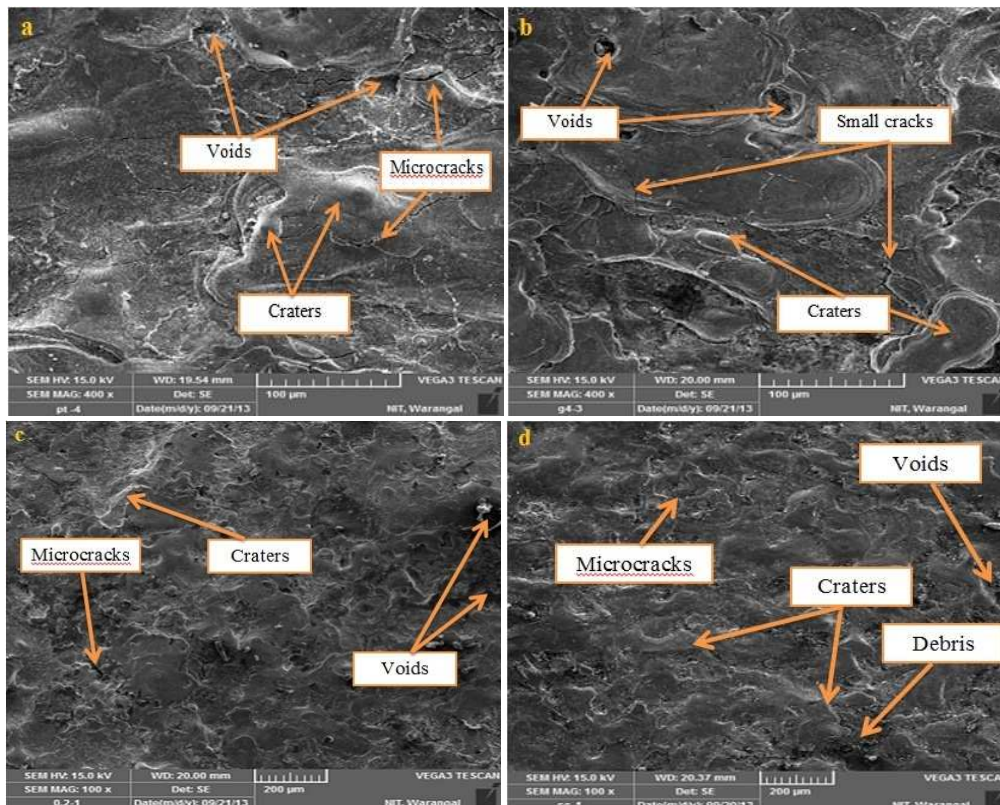


Fig. 8. SEM micrographs of machining surfaces of MRR (a-b) and SR (c-d) in (6 C-45  $P_{on}$ -40  $P_{off}$ -50 V) & (8 C-60  $P_{on}$ -55  $P_{off}$ -60 V) conditions

This results in huge amounts of molten material and floating metal being suspended in the machining zone, resulting in formation of deep and overlapping craters. The formation of micro cracks on the surface is attributed to the presence of thermal stress and tensile stress [11].

The SEM micrographs taken of the SR specimens reveal different sizes of small craters, particle debris, various irregularities on the machined surfaces, various sizes of microcracks and minor voids.

This is shown in Figure 8c-d. Because of the lower input current, the different sizes of the machining gap which results in the formation of smaller craters on the machined surface. Therefore, a decrease in pulse energy will lead to smaller craters on the machined surface, as evidenced by the size of the craters [11].

## CONCLUSIONS

Al7010-2%B<sub>4</sub>C-2%BN HMMNC was effectively fabricated by the UASC method and the following results were obtained by EDM.

- The process parameters of the EDM, like the input current,  $P_{on}$ ,  $P_{off}$  and gap voltage were observed to have a significant effect on the output factors like MRR, SR, and TWR.
- The highest MRR values were found at higher levels of  $I_p$  (8) and  $P_{on}$  (60), and average parameters of  $P_{off}$  (25) and  $V$  (40).
- The smallest SR values were observed at lower input conditions, i.e.  $I_p$  (2),  $P_{on}$  (15),  $P_{off}$  (10) and  $V$  (30).
- The smallest TWR values were obtained using higher  $I_p$  (2) and  $P_{on}$  (15) parameters; lower  $P_{off}$  (55) and  $V$  (60) parameters.
- The surface morphology revealed that higher  $P_{on}$  and  $I_p$  had a greater influence on the EDM machined surface as large voids, craters and microcracks were found.

## REFERENCES

- [1] Dirisenapu G., Reddy S.P., Dumpala L., The effect of B4C and BN nanoparticles on the mechanical and microstructural properties of Al7010 hybrid metal matrix, *Materials Research Express* 2019, Sep, 4, 6(10), 105089.
- [2] Gostariani R., Asadabad M.A., Paydar M.H., Ebrahimi R., Morphological and phase evaluation of Al/15 wt.% BN nanocomposite synthesized by planetary ball mill and sintering, *Advanced Powder Technology* 2017, Sep, 1, 28(9), 2232-2238.
- [3] Firestein K.L., Steinman A.E., Golovin I.S., Cifre J., Obraztsova E.A., Matveev A.T., Kowalski A.M., Lebedev O.I., Shtansky D.V., Golberg D., Fabrication, characterization, and mechanical properties of spark plasma sintered Al-BN nanoparticle composites, *Materials Science and Engineering A*, 2015, Aug, 26, 642, 104-112.
- [4] Ezatpour H.R., Parizi M.T., Sajjadi S.A., Ebrahimi G.R., Chaichi A., Microstructure, mechanical analysis and optimal selection of 7075 aluminium alloy based composite reinforced with alumina nanoparticles, *Materials Chemistry and Physics* 2016, Aug, 1, 178, 119-127.
- [5] Wang L., Qiu F., Zou Q., Yang D.L., Tang J., Gao Y.Y., Li Q., Han X., Shu S.L., Chang F., Jiang Q.C., Microstructures and tensile properties of nano-sized SiCp/Al-Cu composites fabricated by semisolid stirring assisted with hot extrusion, *Materials Characterization* 2017, Sep, 1, 131, 195-200.
- [6] Pal A., Poria S., Sutradhar G., Sahoo P., Tribological behaviour of Al-WC nano-composites fabricated by ultrasonic cavitation assisted stir-cast method, *Materials Research Express* 2018, Mar, 28, 5(3), 036521.
- [7] Poovazhagan L., Kalaichelvan K., Sornakumar T., Processing and performance characteristics of aluminium-nano boron carbide metal matrix nanocomposites, *Materials and Manufacturing Processes* 2016, Jul, 26, 31(10), 1275-1285.
- [8] Madhukar P., Selvaraj N., Gujjala R., Rao C.S., Production of high-performance AA7150-1% SiC nanocomposite by novel fabrication process of ultrasonication-assisted stir casting, *Ultrasonics Sonochemistry* 2019, Nov, 1, 58, 104665.
- [9] Kolli M., Kumar A., Surfactant and graphite powder-assisted electrical discharge machining of titanium alloy, *Proceedings of the Institution of Mechanical Engineers, Journal of Engineering Manufacture Part B*, 2017 Mar, 231(4), 641-657.
- [10] Velmurugan C., Subramanian R., Thirugnanam S., Anandavel B., Experimental investigations on machining characteristics of Al 6061 hybrid metal matrix composites processed by electrical discharge machining, *International Journal of Engineering, Science and Technology* 2011, 3(8), 87-101.
- [11] Kumar S.S., Uthayakumar M., Kumaran S.T., Parameswaran P., Electrical discharge machining of Al (6351)-SiC-B4C hybrid composite, *Materials and Manufacturing Processes* 2014, Dec, 2, 29(11-12), 1395-1400.
- [12] Senthilkumar V., Omprakash B.U., Effect of titanium carbide particle addition in the aluminium composite on EDM process parameters, *Journal of Manufacturing Processes* 2011, Jan, 1, 13(1), 60-66.
- [13] Jabbaripour B., Sadeghi M.H., Faridvand S., Shabgard M.R., Investigating the effects of EDM parameters on surface integrity, MRR and TWR in the machining of Ti-6Al-4V, *Machining Science and Technology* 2012, Jul, 1, 16(3), 419-444.
- [14] Katamreddy S.C., Punnath N., Radhika N., Multi-response optimisation of machining parameters in electrical discharge machining of Al LM25/AIB2 functionally graded composite using grey relation analysis, *International Journal of Machining and Machinability of Materials* 2018, 20(3), 193-213.
- [15] Singh M., Dhuria G., Garg H., Multi response optimization of parameters in electric discharge machining of Al/SiC-graphite hybrid composite using grey relational analysis, *International Journal for Science and Emerging Technologies with Latest Trends* 2015, 2(1), 2029-2035.
- [16] Murthy I.N., Rao D.V., Rao J.B., Microstructure and mechanical properties of aluminium-fly ash nanocomposites made by ultrasonic method, *Materials & Design* 2012 Mar, 1, 35, 55-65.
- [17] Kannan C., Vijayakumar T., Karunakaran C., Optimization of process parameters for electro discharge machining of Al 7075-Al<sub>2</sub>O<sub>3</sub> nano composite using different electrode materials, *SAE Technical Paper* 2018, Jul, 9.
- [18] Singh S., Bhardwaj A., Review to EDM by using water and powder-mixed dielectric fluid, *Journal of Minerals and Materials Characterization and Engineering* 2011, Feb, 10, 10(02), 199.
- [19] Pramanik A., Electrical discharge machining of MMCs reinforced with very small particles, *Materials and Manufacturing Processes* 2016, Mar, 11, 31(4), 397-404.